Letters on Materials 11 (2), 2021 pp. 164-169 www.lettersonmaterials.com

https://doi.org/10.22226/2410-3535-2021-2-164-169 PACS: 72.80.Tm, 81.20.-n, 81.20.Ka

Thermal behavior of Ni-doped $CaCu_3Ti_4O_{12}$ ceramics

N. A. Zhuk†,1, V. A. Belyy[2], E. U. Ipatova[2], T. K. Rocheva[2], I. V. Gruzdev[3], M. M. Ignatova[1]

†nzhuck@mail.ru

[1]Syktyvkar State University, Syktyvkar, 167001, Russia
[2]Institute of Chemistry of the Komi Science Center UB RAS, Syktyvkar, 167982, Russia
[3]Institute of Biology of the Komi Science Center UB RAS, Syktyvkar, 167982, Russia

The calcium-copper titanate has attracted the attention of scientists in connection with the manifestation of gigantic values of permittivity in a wide frequency (10^2–10^6 Hz) and temperature ranges (100 – 600 K), while not being a ferroelectric. In this article, we report on the results of studies of the thermal behavior of Ni-doped CCTO by thermal analysis methods. The interest in this work is due, first of all, to the fact that earlier, for iron-containing compounds, we found a reproducible low-temperature exothermic effect in the temperature range of 506 – 573 K, the nature of which has not been fully elucidated. It is only known that such a behavior of ceramics is recorded by the impedance spectroscopy data, it is not associated with the phase transition and is weaker for an undoped CCTO. Samples of Ni-doped $CaCu_3Ti_4O_{12}$ ceramics of the composition $CaCu_3Ti_4\text{-}4_xNi_{4x}O_{12-\delta}$ and $CaCu_{3-3x}Ni_{3x}Ti_4O_{12}$ ($x = 0.005$, 0.01, 0.02, 0.03, 0.04, 0.06) were obtained by the solid-phase synthesis method. According to the XRD results, copper (II) oxide may be present in trace amounts in all samples. The X-ray picture of $CaCu_3Ti_{4-4x}Ni_{4x}O_{12-\delta}$ samples ($x \geq 0.04$) revealed calcium titanate reflexes. The thermal behavior of the samples was studied by DSC and thermogravimetry methods up to 1323 K. The reproduced exothermic effect in the temperature range 487 – 653 K and endothermic at 1269 K (1285 K) for $CaCu_{3-3x}Ni_{3x}Ti_4O_{12}$ ($CaCu_3Ti_{4-4x}Ni_{4x}O_{12-\delta}$) are observed on the DSC curves of the synthesized samples of both series, associated with thermal dissociation of CuO impurities. Thermogravimetric curves in both cases show a mass loss of samples of no more than 0.35 mass.%. Samples analyzed by FTIR and mass spectrometry.

Keywords: thermal analysis, calcium-copper titanate, nickel.

УДК: 537.3, 537.9, 538.9

Термическое поведение допированного никелем $CaCu_3Ti_4O_{12}$

Жук Н. А.†,1, Белый В. А.[2], Ипатова Е. У.[2], Рочева Т. К.[2], Груздев И. В.[3], Игнатова М. М.[1]

[1]Сыктывкарский государственный университет, Сыктывкар, 167001, Россия
[2]Институт химии Коми НЦ УрО РАН, Сыктывкар, 167982, Россия
[3]Институт биологии Коми НЦ УрО РАН, Сыктывкар, 167982, Россия

Титанат кальция — меди привлек внимание ученых в связи с проявлением гигантских значений диэлектрической проницаемости в широком частотном (10^2–10^6 Гц) и температурном интервалах (100 – 600 К), не являясь сегнетоэлектриком. В настоящей статье мы сообщаем о результатах исследования термического поведения титаната кальция-меди, допированного атомами никеля. Интерес к данной работе обусловлен результатами исследования термических процессов в железосодержащем титанате кальция-меди. Для железосодержащих препаратов обнаружен воспроизводимый низкотемпературный экзотермический эффект в интервале температур 506 – 573 К, природа которого окончательно не установлена. Ранее установлено, что нелинейные свойства керамики фиксируются данными импеданс-спектроскопии, они не связаны с фазовым переходом и слабее проявляются для нелегированного титаната кальция — меди. Методом твердофазного синтеза получены образцы $CaCu_3Ti_4O_{12}$ и $CaCu_3Ti_4\text{-}4_xNi_{4x}O_{12-\delta}$, $CaCu_{3-3x}Ni_{3x}Ti_4O_{12}$ ($x = 0.005$, 0.01, 0.02, 0.03, 0.04, 0.06). Согласно результатам рентгенофазового анализа, во всех образцах присутствует оксид меди (II) в следовых количествах. Для образцов состава $CaCu_3Ti_{4-4x}Ni_{4x}O_{12-\delta}$ ($x \geq 0.04$) выявлены рефлексы титаната кальция. Термическое поведение образцов обеих серий исследовали методами дифференциальной сканирующей калориметрии (ДСК) и термогравиметрии до температуры 1323 К. На кривых ДСК синтезированных образцов обеих серий наблюдаются воспроизводимые экзотермический эффект в интервале температур 487 – 653 К и эндотермический при 1269 К (1285 К) для $CaCu_3Ti_{4-4x}Ni_{4x}O_{12-\delta}$ и $CaCu_{3-3x}Ni_{3x}Ti_4O_{12}$ соответственно, связанный с термической диссоциацией примеси CuO. Термогравиметрические кривые в обоих случаях показывают потерю массы образцов не превышающей 0.35 мас.%. Показаны результаты анализа образцов методом ИК- и масс-спектрометрии.

Ключевые слова: термический анализ, титанат кальция-меди, никель.

1. Introduction

To this day, calcium-copper titanate has attracted the attention of scientists in connection with the manifestation of gigantic values of permittivity ($\varepsilon \sim 10^4 - 10^5$) in a wide frequency ($10^2 - 10^6$ Hz) and temperature ranges (100 – 600 K), while not being a ferroelectric [1, 2]. Calcium-copper titanate was discovered by A. Deschanvres et al in 1967, and its properties were studied in detail by M. A. Subramanian et al. [1 – 3]. The unique behavior of calcium-copper titanate and its related compounds promises the prospect of its widespread use in microelectronics. Materials based on them can be used in the manufacture of multilayer capacitors and microwave devices. High dielectric losses limit the practical use of calcium-copper titanate [4]. The main efforts of scientists are aimed at minimizing dielectric losses, while maintaining high values of permittivity. The main technique that is used to optimize the electrophysical characteristics of CCTO is doping. It has been shown that doping with CCTO is possible both for copper, titanium, and also co-doping [5 – 12]. Good dielectric properties are demonstrated by CCTO ceramics doped with nickel atoms. Substitution of copper atoms with nickel atoms leads to an increase in the dielectric constant of calcium-copper titanate and, in some cases, to a decrease in the dielectric loss tangent [9,11,12]. As reported by J. Wang et al. [11] the best electrophysical characteristics are ceramic CCTO, in which 20 mol.% of copper atoms is replaced by nickel. Such ceramics exhibits a dielectric constant of $1.51 \cdot 10^5$ and a dielectric loss tangent of 0.051 at room temperature and a frequency of 1 kHz. Rai et al. [13] when comparing the dielectric properties of ceramics $CaCu_{2.9}Ni_{0.1}Ti_4O_{12}$ and $CaCu_3Ti_{3.9}Ni_{0.1}O_{12}$, it was found that $CaCu_{2.9}Ni_{0.1}Ti_4O_{12}$ is characterized by higher dielectric constant and dielectric loss. The research results show that the dielectric properties of Ni-doped CCTO are highly dependent on sample preparation, synthesis method, and sintering conditions. In the course of studies, it was found that nickel atoms predominantly replace Cu positions in CCTO at concentrations not exceeding $x = 0.3$ for $CaCu_{3-x}Ni_xTi_4O_{12}$ [6, 9,10,12]. Ceramics $CaCu_3Ti_4O_{12-x}$NiO exhibits increased density and accelerated grain growth [5, 9].

From time to time, the question arises about the presence of a high-temperature phase transition of calcium-copper titanate and its solid solutions in connection with the possibility of the manifestation of various relaxation processes in them. A. Onodera et al. [14,15], basing on the analysis of the results of structural, calorimetric and dielectric studies, concluded that at 732 K a structural phase transition can be observed. Later, M. V. Gorev et al. [16], in the study of thermal expansion and heat capacity of CCTO, refuted this possibility, indicating the monotonicity of changes in thermal expansion in the range of 120 – 1200 K ($\alpha(T) = 5 \cdot 10^{-5} - 11 \cdot 10^{-6}$ K^{-1}), which does not contradict the results of studies of other scientists [17]. Meanwhile, an anomaly of thermal expansion was noted during cooling of the sample (at 850 and 950 K) and was associated with a variation in the stoichiometry of the composition of the surface layer of grain in ceramic samples. By Zhang M. N. et al. [18] based on studies of the dielectric properties of $CaCu_3Ti_4O_{12}$ up to 1073 K and in the frequency range 20 Hz – 10 MHz, three dielectric anomalies were detected that are sensitive to the sintering conditions and the annealing atmosphere of the sample, which indicates, according to the authors, their dependence on the contact of the electrode with the sample and oxygen vacancies.

In this article, we report on the results of studies of the thermal behavior of Ni-doped CCTO by thermal analysis methods. The interest in this work is due, first of all, to the fact that earlier, for iron-containing compounds, we found a reproducible low-temperature exothermic effect in the temperature range of 506 – 573 K, the nature of which has not been fully elucidated. It is only known that such a behavior of ceramics is recorded by impedance spectroscopy data, it is not associated with a phase transition and is weaker for an undoped CCTO.

2. Experimental part

The solid solution samples $CaCu_3Ti_{4-4x}Ni_{4x}O_{12-\delta}$ and $CaCu_{3-3x}Ni_{3x}Ti_4O_{12}$ ($x = 0.005$, 0.01, 0.02, 0.03, 0.04, 0.06) were obtained via the standard ceramic procedure from “special pure” grade $CaCO_3$ and Ni (II), Ti (IV), Cu (II) oxides using staged calcination at 923, 1123, 1223 and 1323 K. The synthesis technology was the same for the samples of both series.

The phase composition of the samples was monitored by means of X-ray phase analysis (a DRON-4-13 diffractometer, CuK$_\alpha$ emission) and scanning electron microscopy (electron scanning microscope Tescan VEGA 3LMN, energy dispersion spectrometer INCA Energy 450). The unit-cell parameters were calculated by Pawley approach using Topas 5.0 [19].

Thermal analysis of the samples of $CaCu_3Ti_{4-4x}Ni_{4x}O_{12-\delta}$ and $CaCu_{3-3x}Ni_{3x}Ti_4O_{12}$ was carried out by means of a simultaneous thermal analyzer STA 409 PC Luxx (Netzsch, Germany) in the dynamic air atmosphere at the heating rate of 10 K/min in platinum crucibles. The measurements were carried out in a furnace with Pt-PtRh thermocouples of in the temperature range of 293 ÷ 1323 K and 293 ÷ 723 ÷ 373 K. The rate of 10 K/min was chosen because it allowed to register well resolved thermal effects and to be closer to the thermodynamic equilibrium in the sample without significant extending of the time of experiment. Air was the purge gas, the flow was 20 ml/min. An empty crucible was used as a reference. The relative standard deviation of the determination of the temperatures and enthalpy of phase transitions of the calibration substances was 0.5%. To calibrate the temperature and enthalpy sensitivities of the TG-DSC instrument, a DSC/DTA calibration kit was used (Netzsch 6.223.5 – 91.2). The following standard compounds with the corresponding phase transition temperatures were used for the calibration: C_6H_5COOH (395.4 K), $KClO_4$ (573.8 K), Ag_2SO_4 (699.2 K), K_2CrO_4 (941.0 K), $BaCO_3$ (1081.0 K). About ≈ 60 mg of a calibration standard weighted with the accuracy of ±0.001 mg were placed in a Pt crucible with a perforated lid. An empty Pt crucible with a perforated lid was used as a reference. The heating rate was 10 K per minute. TG and DSC curves were registered. This procedure was repeated three times for each calibration substance. The values of enthalpy and onset temperatures of the endothermic effects of the calibration substances were measured in NETZSCH Proteus software and used for making the calibration curves.

Fourier transform infrared (FTIR) spectra were recorded on a IRPrestige-21 Shimadzu (Japan) spectrophotometer equipped with a DLATGS detector in the wavenumber range of 400 – 4000 cm^{-1} with a resolution of 4 cm^{-1}. Before analysis, the samples were mixed and ground with KBr (2% of a sample by weight). The transmission spectra were obtained using the diffuse reflection mode. The data were processed using the Shimadzu software.

Mass spectrometric analysis was carried out on a DSQ mass spectrometer (Thermo, USA) in the electron impact mode (electron energy 70 eV, mass scanning in the range of 10 – 1050 Da) using the Xcalibur Data System software and the NIST05 mass spectra library. The samples were injected directly into the ionization source in a micro crucible (DIP) and heated from 50°C to 350°C at a rate of 30°C/min under vacuum (70 mTorr).

3. Results and discussion

3.1. Phase composition and microstructure of samples

Samples of the compositions $CaCu_{3-3x}Ni_{3x}Ti_4O_{12}$ and $CaCu_3Ti_{4-4x}Ni_{4x}O_{12-\delta}$ ($x \leq 0.06$) were studied by X-ray phase analysis (XRD) and electron scanning microscopy (Fig. S1, supplementary material). Based on the XRD analysis, it was found that the samples crystallize in the cubic structure of $CaCu_3Ti_4O_{12}$ described by the space group (Im-3) [1 – 3]. On the X-ray diffraction patterns of the preparations of both series, trace amounts of the impurity phase of copper (II) oxide are recorded [11, 20 – 22], with slightly more CuO in $CaCu_3Ti_{4-4x}Ni_{4x}O_{12-\delta}$. We believe that this may be due to the tendency of nickel (II) atoms to occupy the coordination positions of copper (II), which has a square plane geometry [3].

Impurities of nickel oxide in the samples of both series in the entire studied concentration range by X-ray powder diffraction and electron scanning microscopy were not recorded. X-ray diffraction patterns of $CaCu_3Ti_{4-4x}Ni_{4x}O_{12-\delta}$ samples at $x \geq 0.04$ show $CaTiO_3$ impurity reflections, in contrast to $CaCu_{3-3x}Ni_{3x}Ti_4O_{12}$, which indicates the limited solubility of nickel (II) oxide in CCTO and the predominant distribution of nickel (II) ions in Cu (II) positions.

The unit cell parameter of $CaCu_3Ti_4O_{12}$ is 7.3881 Å [20]. For $CaCu_{3-3x}Ni_{3x}Ti_4O_{12}$ samples, the parameter is close to the calcium-copper titanate parameter: 7.3921 ($x = 0.010$) and 7.39116 Å ($x = 0.06$). The cell parameter of the $CaCu_3Ti_{4-4x}Ni_{4x}O_{12-\delta}$ samples varies from 7.3921 ($x = 0.010$) to 7.3941 Å ($x = 0.06$), which does not contradict the literature [11].

The method of electron scanning microscopy of samples of both series of substituted calcium-copper titanate confirmed the formation of nickel-containing solid solutions. However, in micrographs of samples of both series, copper (II) oxide is observed in the intergrain space (bright areas). Due to the fact that copper (II) oxide is observed in the samples of both series, it can be concluded that the yield of copper oxide is due to a long heat treatment (20 h) at 1323 K [21, 22]. Samples of both series of solid solutions are compacts consisting of fused melted grains ranging in size from 2 to 9 μm (Figs. S1-S3, supplementary material). In the EDS spectra of samples of both series (Fig. S1, supplementary material), the intensity of the absorption line from nickel atoms increases with increasing formula content of nickel in the sample formula, which confirms the conclusion that nickel dissolves in calcium-copper titanate in the concentration range under consideration.

3.2. Thermal analysis

The synthesized samples of Ni-doped $CaCu_3Ti_4O_{12}$ ceramics were studied by thermal analysis methods (DSC and TG) in the heating mode with a step of 10 deg/min in the temperature range 293 – 1323 K (Fig. 1).

It should be noted that for samples of both $CaCu_{3-3x}Ni_{3x}Ti_4O_{12}$ and $CaCu_3Ti_{4-4x}Ni_{4x}O_{12-\delta}$ ($x = 0.03$) the behavior of the TG and DSC curves, in general, coincides. Two effects are recorded on the DSC curves: exothermic in the range of 487 – 653 K and endothermic at 1269 K (1285 K) for $CaCu_{3-3x}Ni_{3x}Ti_4O_{12}$ ($CaCu_3Ti_{4-4x}Ni_{4x}O_{12-\delta}$) with a slight weight loss of up to 0.35 mass.%. It is interesting to note that the low-temperature effect manifests itself as an overlap of two successively occurring exothermic effects at ≈531 K and 576 – 598 K. The thermal effect of the low-temperature thermal transformation in both cases is two times different on average and does not show a clear dependence on the sample weighed for analysis: $CaCu_{2.91}Ni_{0.09}Ti_4O_{12}$ (55.44 mg) and $CaCu_3Ti_{3.88}Ni_{0.12}O_{12-\delta}$ (65.38 mg). Moreover, as will be shown below, it also does not depend on the content of impurity copper (II) oxide. We can only state that in the same temperature range (506 – 573 K) the uncomplicated exothermic effect of Fe-doped $CaCu_3Ti_4O_{12}$ is exhibited [23].

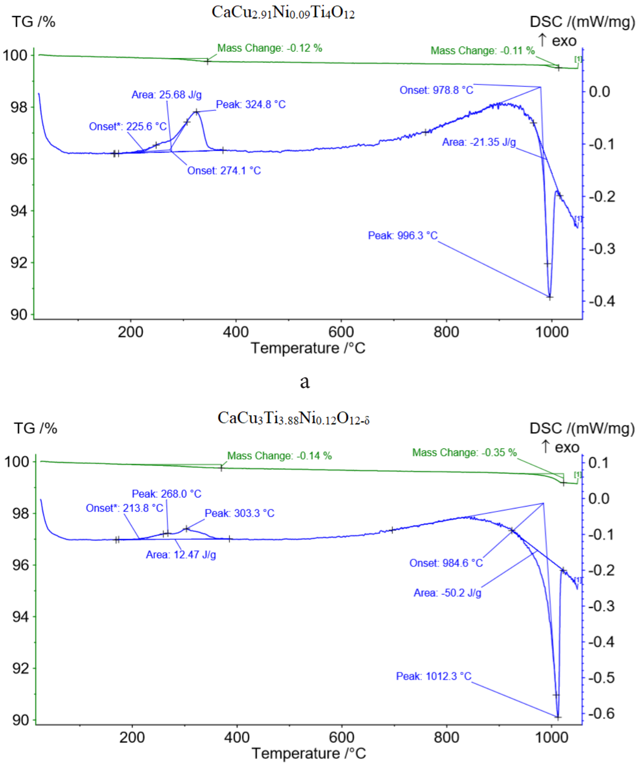

Fig. 1. (Color online) TG and DSC curves of the $CaCu_{2.91}Ni_{0.09}Ti_4O_{12}$ (a) and $CaCu_3Ti_{3.88}Ni_{0.12}O_{12-\delta}$ (b).

We hypothesized that the observed exothermic effect could be related to samples storage and CO_2 or H_2O sorption. As a result, we performed a two-time continuous thermal analysis in the range of 293 – 723 – 373 K in the heating-cooling mode of the sample (Fig. 2).

From Fig. 2 we can see that freshly calcined samples of exothermic effect do not show, which confirms our hypothesis about their sorption of volatile components from the air. Two weeks after the last experiment, we again investigated the thermal behavior of the analyzed samples. As a result, it was found that for both series of samples, the exothermic effect is again manifested within the specified temperature range (Fig. S4, supplementary material). On the basis of our studies, we concluded that the low-temperature exothermic effect is not related to the phase transformation of CCTO, it is reproduced for samples stored in the air and is accompanied by a slight mass loss of the sample [24,25]. The assumption of sorption of volatile components, e. g., water vapors, was tested by infrared spectroscopy of the samples (below).

The high-temperature endothermic effect manifests itself at 1269 K (1285 K) for $CaCu_{3-3x}Ni_{3x}Ti_4O_{12}$ ($CaCu_3Ti_{4-4x}Ni_{4x}O_{12-\delta}$) and it is similar to that observed previously for calcium-copper titanate [21]. The high-temperature endothermic effect is apparently caused by the thermal dissociation of copper (II) oxide according to the reaction equation: $2CuO \rightarrow ½O_2 + Cu_2O$.

According to [26], the reaction proceeds at 1326 K, but due to the X-ray amorphous state of copper (II) oxide segregated in the intergranular space of CCTO ceramic, the process temperature may be lower. For an iron-containing preparation, this transformation is recorded by the DSC method in the temperature range (1256 – 1259 K), and for undoped calcium-copper titanate ≈1250 K. The thermal effect of the process for samples of both series is significantly different. A simple algebraic calculation shows that the thermal effect in $CaCu_3Ti_{3.88}Ni_{0.12}O_{12-\delta}$ is 2.7 times higher than the expected value, which can be associated either with an uneven content of copper oxide impurity in the samples or with a high content of CuO impurity in $CaCu_3Ti_{4-4x}Ni_{4x}O_{12-\delta}$ samples. By the magnitude of the thermal effect, we can estimate the content of copper oxide in the samples. Knowing the standard enthalpy of the Cu (II) → Cu (I) process ($\Delta H_{298} = 75.5$ kJ/mol, [26]), the amount of decomposed copper (II) oxide can be calculated for each case from the value of the thermal effect (or from the mass fraction of losses) samples of the composition $CaCu_{2.91}Ni_{0.09}Ti_4O_{12}$ and $CaCu_3Ti_{3.88}Ni_{0.12}O_{12-\delta}$. As a result of the calculation, it was found that the composition of the first sample corresponds to the approximate formula $CaCu_{2.83}Ni_{0.09}Ti_4O_{11.92} - 0.08CuO$ and the second — $CaCu_{2.73}Ti_{3.88}Ni_{0.12}O_{12-\delta} - 0.27CuO$, i. e. only 2.8 and 9.0 molar percent of copper (II) oxide of the total copper content in Ni-doped CCTO ceramics.

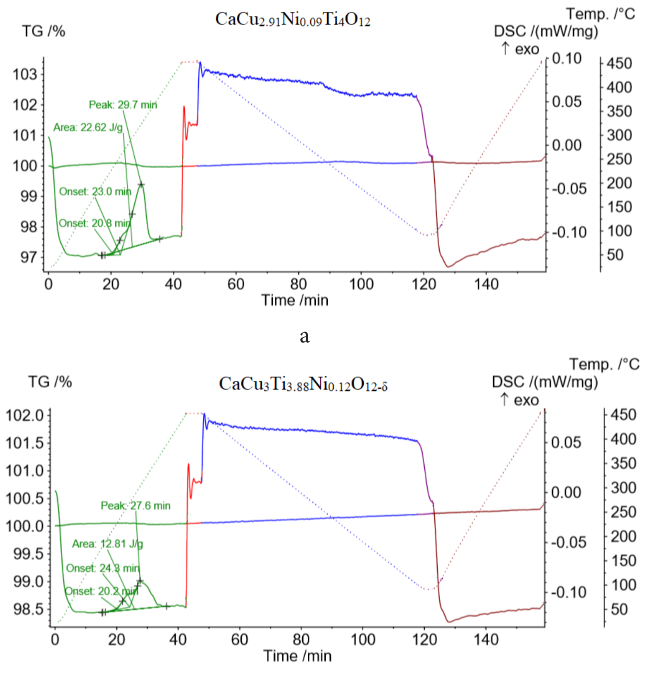

a

b

Fig. 2. (Color online) TG and DSC curves of the $CaCu_{2.91}Ni_{0.09}Ti_4O_{12}$ (a) and $CaCu_3Ti_{3.88}Ni_{0.12}O_{12-\delta}$ (b) in the range of 293 – 723 – 373 K.

3.3. FTIR and mass spectrometry

FTIR spectra of CCTO and solid solutions of the $CaCu_{3-3x}Ni_{3x}Ti_4O_{12}$ and $CaCu_3Ti_{4-4x}Ni_{4x}O_{12-\delta}$ ($x = 0.03$) before and after calcination (at 723 K) were obtained (Figs. 3, S5, supplementary material).

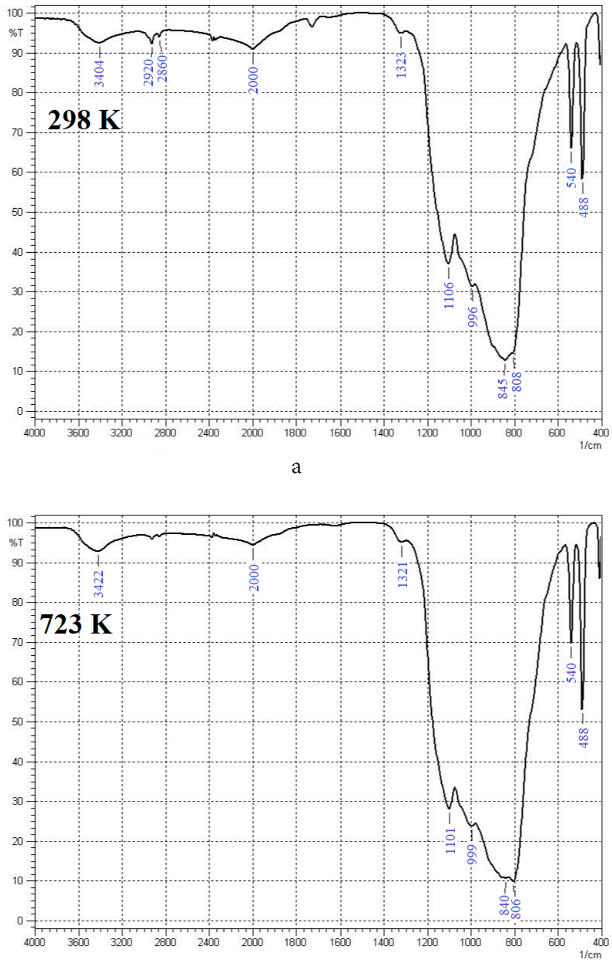

a

b

Fig. 3. (Color online) Comparison of FTIR spectra of the $CaCu_{3-3x}Ni_{3x}Ti_4O_{12}$ samples stored in the air at 298 K (a) with samples calcinated at temperature of 723 K for 180 min (b).

IR spectra of the samples are recorded in a matrix of potassium bromide in a frequency range of 400 – 4000 cm^{-1}. The attribution of observed absorption bands is made on the basis of literature data [27 – 32]. The main components of CCTO and Ni-doped CCTO IR spectra are reproduced with the data given in the literature. On spectra of all samples three absorption bands in the area of fingerprints at ≈410, 488 – 490, 540 cm^{-1}, connected according to data [27, 28] with valence oscillations TiOTi (410), Cu-O (≈489) and Ca-O bonds at 540 cm^{-1} in CCTO are clearly fixed. The authors of [29, 30] connect the absorption bands at 540 and 489 cm^{-1} with the valence oscillations of TiO bond in the octahedron TiO_6. The wide diffuse absorption band in the region of 600 – 1200 cm^{-1}, typical for CCTO and Ni-doped CCTO, observed earlier in works [30] and [31], attracts attention. On its background, the maximums at 1099 – 1105, 995 – 999, 840 – 852, 802 – 806 cm^{-1}, which can be associated with vibrations of CuO_4, TiO_6 groups, are clearly seen [27, 32]. No absorption bands typical for carbonate ions and water molecules were found in the spectra of samples before and after calcination [32]. On the other hand, visible changes in the spectra for all calcined samples appear against the background of the diffuse band, it becomes wider, probably due to a decrease in the intensity of the bands 840 – 852, 802 – 806 cm^{-1} and an increase in the intensity of the bands manifested in the shoulder form in the interval 600 – 800 cm^{-1}. This behavior may be related to the thermal activation and diffusion of oxygen atoms, which affects the distortion of TiO_6 polyhedrons and TiO coupling oscillations. After calcination of the Ni-doped CCTO samples, there is a decrease in the intensity of the absorption line at 2400 cm^{-1}, which referred to air. The absorption band of deformation oscillations of H_2O was not detected. We assume that such spectrum changes may be related to this behavior may be related to the thermal activation and diffusion of oxygen atoms.

An analysis of the behavior of the $CaCu_3Ti_{4-4x}Ni_{4x}O_{12-\delta}$ and $CaCu_{3-3x}Ni_{3x}Ti_4O_{12}$ and CCTO samples by mass spectrometry in the temperature range 323 – 623 K did not allow us to establish the nature of the released component. When heated in the temperature range from 323 to 623 K under vacuum (70 mTorr), the analyzed sample (Fig. S6, supplementary material) does not emit compounds with masses in the range of 10 – 1050 Da.

4. Conclusion

As a result of investigation of the thermal behavior of $CaCu_3Ti_{4-4x}Ni_{4x}O_{12-\delta}$ and $CaCu_{3-3x}Ni_{3x}Ti_4O_{12}$ samples by thermal analysis methods up to 1323 K, two reproducible thermal transformations in the range of 487 – 653 K and near 1275 K were established. With the exothermic effect, a comparable mass loss of samples of both series was fixed, not exceeding 0.14 mass.%. Based on the analysis of FTIR, MS spectra of the samples, it is supposed that the exothermic effect is connected with the diffusion of oxygen atoms. The endothermic effect is associated with thermal dissociation of copper oxide (II) and is accompanied by a slight mass loss. According to thermal analysis, the CuO content in $CaCu_3Ti_{4-4x}Ni_{4x}O_{12-\delta}$ samples is significantly higher than in $CaCu_{3-3x}Ni_{3x}Ti_4O_{12}$.

Supplementary material. *The online version of this paper contains supplementary material available free of charge at the journal's Web site (lettersonmaterials.com).*

References

1. M.A. Subramanian, D. Li, N. Duan, B.A. Reisner, A.W. Sleight. J. Sol. St. Chem. 151, 323 (2000). Crossref
2. H.E. Kim, S.-D. Yang, J.-W. Lee, H.M. Park, S.-I. Yoo. J. Cryst. Growth. 408, 60 (2014). Crossref
3. A. Deschanvres, B. Raveau, F. Tollemer. Bull. Soc. Chim. Fr. 11, 4077 (1967).
4. M. Ahmadipour, M.F. Ain, Z.A. Ahmad. Nano-Micro Lett. 8, 291 (2016). Crossref
5. F. Gaâbel, M. Khlifi, N. Hamdaoui, K. Taibi, J. Dhahri. J. Alloy. Compd. 828, 154373 (2020). Crossref
6. T. Moriyama, A. Kan, H. Ogawa. Mater. Sci. Eng. B. 178, 875 (2013). Crossref
7. S. Kwon, C.-C. Huang, E.A. Patterson, D.P. Cann, E.F. Alberta, S. Kwon, W.S. Hackenberger, D.P. Cann. Mater. Lett. 62, 633 (2008). Crossref
8. C. Xu, X. Zhao, L. Ren, J. Sun, L. Yang, J. Guo, R. Liao. J. Alloys Comp. 792, 1079 (2019). Crossref
9. L. Sun, R. Zhang, Z. Wang, E. Cao, Y. Zhang, L. Ju. RSC Advances. 6, 55984 (2016). Crossref
10. T. Li, J. Chen, D. Liu, Z. Zhang, Z. Chen, Z. Li, X. Cao, B. Wang. Ceram. Intern. 40, 9061 (2014). Crossref
11. J. Wang, Z. Lu, T. Deng, C. Zhong, Z. Chen. J. Am. Ceram. Soc. 100, 4021 (2017). Crossref
12. S. Senda, S. Rhouma, E. Torkani, A. Megriche, C. Autret. J. Alloys Comp. 698, 152 (2017). Crossref
13. A.K. Rai, K.D. Mandal, D. Kumar, O. Parkash. J. Alloys Comp. 491, 507 (2010). Crossref
14. A. Onodera, K. Kawatani, M. Takesada, M. Oda, M. Ido. Jpn. J. App. Phys. 48, 09KF12 (1-3) (2009). Crossref
15. K. Kawatani, M. Takesada, M. Fukunaga, M. Oda, M. Ido, A. Onodera. Ferroelectrics. 402, 200 (2010). Crossref
16. M.V. Gorev, I.N. Flerov, A.V. Kartashev, S. Guillemet-Fritsch. Phys. Sol. St. 54, 1785 (2012). Crossref
17. X. Li, C. Chen, F. Zhang, X. Huang, Z. Yi. Appl. Phys. Lett. 116, 112901 (2020). Crossref
18. M. Zhang, K. Xu, G. Wang, C. Wang. Chin. Sci. Bull. 58, 713 (2013). Crossref
19. A.X. S. Bruker. Topas 5.0. General Profile and Structure Analysis Software for Powder Diffraction Data (2014) Karlsruhe, Germany.
20. N.A. Zhuk, S.V. Nekipelov, V.N. Sivkov, B.A. Makeev, R.I. Korolev, V.A. Belyy, M.G. Krzhizhanovskaya, M.M. Ignatova. Mater. Chem. Phys. 252, 123310 (2020). Crossref
21. N.A. Zhuk, S.M. Shugurov, V.A. Belyy, B.A. Makeev, M.V. Yermolina, D.S. Beznosikov, L.A. Koksharova. Ceram. Intern. 44, 20841 (2018). Crossref
22. N.A. Sekushin, N.A. Zhuk, L.A. Koksharova, V.A. Belyy, B.A. Makeev, D.S. Beznosikov, M.V. Yermolina. Letters on Materials. 9 (1), 5 (2019). (in Russian) [Н.А. Секушин, Н.А. Жук, Л.А. Кокшарова, В.А. Белый, Б.А. Макеев, Д.С. Безносиков, М.В. Ермолина. Письма о материалах. 9 (1), 5 (2019).] Crossref

23. N.A. Zhuk, V.P. Lutoev, A.Y. Lysyuk, B.A. Makeev, V.A. Belyy, S.V. Nekipelov et al. J. Alloys Comp. 855, 157400 (2021). Crossref
24. N.A. Zhuk, M.G. Krzhizhanovskaya, V.A. Belyy, N.A. Sekushin, A.I. Chichineva. Scripta Mater. 173, 6 (2019). Crossref
25. N.A. Sekushin, L.A. Koksharova, N.A. Zhuk. Letters on Materials. 10 (1), 72 (2020). (in Russian) [Н.А. Секушин, Л.А. Кокшарова, Н.А. Жук. Письма о материалах.10 (1), 72 (2020).] Crossref
26. R.A. Lidin, V.A. Molochko, L.L. Andreeva. Reactions of inorganic substances: handbook. Moscow, Drofa (2007) 637 p. (in Russian) [Р. А. Лидин, В. А. Молочко, Л. Л. Андреева. Реакции неорганических веществ: Справочник. Москва, Дрофа (2007) 637 с.]
27. S. Jesurani, S. Kanagesan, R. Velmurugan, T. Kalaivani. J. Mater. Sci.: Mater. Electron. 23, 668 (2011). Crossref
28. N. Hadi, A. Farid, T.-E. Lamcharfi, A. Belaaraj, S. Kassou, F. Ahjyaje. Mediterranean J. Chem. 8, 245 (2019). Crossref
29. L.C. Kretly, A.F. L. Almeida, P.B. A. Fechine, R. S. de Oliveira, A.S. B. Sombra. J. Mater. Sci. Mater. Electron. 15, 657 (2004). Crossref
30. C. Masingboon, S. Maensiri, T. Yamwong, P.L. Anderson, S. Seraphin. Appl. Phys. A. 91, 87 (2007). Crossref
31. A.F. L. Almeida, P.B. A. Fechine, M.P. F. Graça, M.A. Valente, A.S. B. Sombra. J. Mater. Sci.: Mater. Electron. 20, 163 (2008). Crossref
32. P. Thomas, K. Dwarakanath, K.B.R. Varma, T.R.N. Kutty. J. Phys. Chem. Sol. 69, 2594 (2008). Crossref